Video Article

A Mouse Model for Pathogen-induced Chronic Inflammation at Local and Systemic Sites

George Papadopoulos*[1], Carolyn D. Kramer*[1], Connie S. Slocum[1], Ellen O. Weinberg[1], Ning Hua[2], Cynthia V. Gudino[1], James A. Hamilton[1], Caroline A. Genco[1]

[1]Department of Medicine, Section of Infectious Disease, Boston University School of Medicine

[2]Department of Biophysics, Boston University School of Medicine

*These authors contributed equally

Correspondence to: Caroline A. Genco at cgenco@bu.edu

URL: https://www.jove.com/video/51556
DOI: doi:10.3791/51556

Keywords: Immunology, Issue 90, Pathogen-Induced Chronic Inflammation; *Porphyromonas gingivalis*; Oral Bone Loss; Periodontal Disease; Atherosclerosis; Chronic Inflammation; Host-Pathogen Interaction; microCT; MRI

Date Published: 8/8/2014

Citation: Papadopoulos, G., Kramer, C.D., Slocum, C.S., Weinberg, E.O., Hua, N., Gudino, C.V., Hamilton, J.A., Genco, C.A. A Mouse Model for Pathogen-induced Chronic Inflammation at Local and Systemic Sites. *J. Vis. Exp.* (90), e51556, doi:10.3791/51556 (2014).

Abstract

Chronic inflammation is a major driver of pathological tissue damage and a unifying characteristic of many chronic diseases in humans including neoplastic, autoimmune, and chronic inflammatory diseases. Emerging evidence implicates pathogen-induced chronic inflammation in the development and progression of chronic diseases with a wide variety of clinical manifestations. Due to the complex and multifactorial etiology of chronic disease, designing experiments for proof of causality and the establishment of mechanistic links is nearly impossible in humans. An advantage of using animal models is that both genetic and environmental factors that may influence the course of a particular disease can be controlled. Thus, designing relevant animal models of infection represents a key step in identifying host and pathogen specific mechanisms that contribute to chronic inflammation.

Here we describe a mouse model of pathogen-induced chronic inflammation at local and systemic sites following infection with the oral pathogen *Porphyromonas gingivalis*, a bacterium closely associated with human periodontal disease. Oral infection of specific-pathogen free mice induces a local inflammatory response resulting in destruction of tooth supporting alveolar bone, a hallmark of periodontal disease. In an established mouse model of atherosclerosis, infection with *P. gingivalis* accelerates inflammatory plaque deposition within the aortic sinus and innominate artery, accompanied by activation of the vascular endothelium, an increased immune cell infiltrate, and elevated expression of inflammatory mediators within lesions. We detail methodologies for the assessment of inflammation at local and systemic sites. The use of transgenic mice and defined bacterial mutants makes this model particularly suitable for identifying both host and microbial factors involved in the initiation, progression, and outcome of disease. Additionally, the model can be used to screen for novel therapeutic strategies, including vaccination and pharmacological intervention.

Video Link

The video component of this article can be found at https://www.jove.com/video/51556/

Introduction

Chronic inflammation is a major driver of pathological tissue damage and a unifying characteristic of many chronic diseases in humans. These diseases include neoplastic, autoimmune, and chronic inflammatory diseases[1]. The etiology of many chronic diseases remains unclear but is understood to be complex and multifactorial, involving both genetic predisposition and the introduction of environmental factors. While the perpetuators of inflammation remain elusive, the cellular and molecular profiles of immune activation overlap considerably with those patterns observed in host responses to pathogens[2].

Mounting evidence implicates infection with microbial pathogens in the development and progression of chronic inflammation and its diverse clinical manifestations[2,3]. Pathogens can induce and sustain chronic inflammation directly by subverting the host immune system and establishing persistent infections[4]. In the absence of microbial persistence, infection can precipitate chronic inflammation from autoimmune reactions triggered by molecular mimicry to self-antigens, changes in self-antigens that render them immunogenic, or damage that releases previously masked host antigens. Rarely however have specific pathogens been identified as the universal cause of a particular chronic disease. Rather, the majority of available data suggests that pathogens use distinct mechanisms to elicit chronic inflammation with a wide spectrum of clinical manifestations and disease outcomes in the genetically susceptible host[3]. Thus, a detailed understanding of the mechanisms by which specific pathogens induce chronic inflammation may have major implications for public health, as well as treatment and prevention of many chronic diseases.

Although the host and pathogen specific mechanisms contributing to the induction and maintenance of chronic inflammation are poorly understood, advances in modeling of pathogen-induced chronic inflammation have begun to further our understanding of these processes. The *P. gingivalis* oral infection model is a unique, well-characterized mouse model of pathogen-induced chronic inflammation that permits the analysis of host and pathogen specific mechanisms contributing to chronic inflammation at local (oral bone loss) and systemic sites (atherosclerosis)[5,6].

P. gingivalis is a Gram-negative, anaerobic oral pathogen implicated in human periodontal disease, an infection-driven chronic inflammatory disease characterized by the destruction of tooth supporting tissue[7]. In addition to pathology at the initial site of infection, accumulating evidence implicates *P. gingivalis*-induced chronic inflammation in the development and progression of systemic diseases including atherosclerosis[5], a disease characterized by chronic inflammation of the arterial vessel wall. Oral infection of specific-pathogen free mice with *P. gingivalis* induces a local inflammatory response that results in destruction of tooth supporting alveolar bone[8]. *P. gingivalis* can be recovered from the mouths of infected mice up to 42 days post-infection[8] and mice develop high levels of pathogen-specific serum antibody titers[9]. In an established mouse model of atherosclerosis using Apolipoprotein-E$^{-/-}$ mice (ApoE$^{-/-}$), oral infection with *P. gingivalis* induces chronic inflammation that drives inflammatory plaque deposition within the aortic sinus[10] and the innominate artery[11]. Progressive inflammation within the innominate artery of *P. gingivalis*-infected mice can be monitored in live animals using *in vivo* MRI. Histologically, arterial lesions from *P. gingivalis*-infected mice exhibit increased accumulation of lipids accompanied by activation of the vascular endothelium, an increased immune cell infiltrate, and elevated expression of inflammatory mediators[12]. Use of this model in knockout mice has elucidated the role of host signaling components and inflammatory mediators, as well as the cell specific interactions that drive *P. gingivalis*-induced immunopathology[12–14]. In addition, experiments utilizing defined bacterial mutants have identified critical *P. gingivalis* virulence factors contributing to chronic inflammation at local and systemic sites[15].

This article details methodologies for the assessment of *P. gingivalis*-induced chronic inflammation at local and systemic sites. We provide a detailed protocol for the analysis of alveolar bone loss by microCT using Amira software. In addition, we define the utility of serial *in vivo* live animal MRI for the assessment of progressive inflammation within the innominate artery. We include methodologies for the visualization and quantification of inflammatory plaque in arterial lesions, and describe their histological characterization. The use of transgenic mice and defined bacterial mutants makes this model particularly suitable for identifying both host and microbial factors involved in the initiation, progression, and outcome of disease. Additionally, the model can be used to screen for novel therapeutic strategies, including vaccination and pharmacological intervention.

Protocol

1. Growth and Cultivation of Bacteria

1. Streak frozen stocks of *P. gingivalis* 381 onto anaerobic blood agar plates and incubate for 3 - 5 days in an anaerobic chamber (10% H_2/10% CO_2/80% N_2) at 37 °C.
2. Use the plate-grown organisms to inoculate 5 ml liquid cultures of brain heart infusion broth (BHI) supplemented with yeast extract (0.5%), hemin (10 µg/ml), and menadione (1 µg/ml). Following O/N growth, transfer the 5 ml cultures into 45 ml of BHI.
3. Incubate the 50 ml liquid cultures anaerobically for an additional18 – 24 hr and harvest at mid to late log phase. NOTE Purity of the culture should always be verified by Gram stain before introducing bacteria into animals.
4. Harvest the bacteria by centrifugation at 7,000 x g for 10 min. Aspirate the supernatant and thoroughly resuspend the bacterial cell pellet in 5 ml PBS using a serological pipet. Add an additional 45 ml of PBS and centrifuge at 7,000 x g for 10 min. Repeat this step twice for a total of three washes.
5. After the last wash, resuspend the cell pellet in PBS such that a 1:10 dilution of the culture has an optical density of 1.0 at 660 nm (an $O.D._{660}$ of 1 is equivalent to 10^9 CFU/ml). Weigh out enough carboxymethyl cellulose (medium viscocity) to achieve a 2% w/v solution (*e.g.,* 0.1 g per 5 ml of culture). Slowly add the carboxymethyl cellulose to the bacterial suspension while vortexing in order to avoid clumping.

2. Oral Infection

NOTE: As illustrated in **Figure 1**, using the appropriate mouse model and oral infection regimen, *P. gingivalis* induces chronic inflammation and immunopathology at local (oral cavity) and systemic sites (arteries).

1. Administer sulfamethoxazole (0.87 mg/ml) and trimethoprim (0.17 mg/ml) (Sulfatrim) to six- to 8-wk-old male mice *ad libitum* in their drinking water for 2 weeks to reduce the normal flora. Keep the antibiotic solution in amber glass bottles and protect it from light to prevent degradation.
2. To avoid sedimentation of the antibiotic solution, shake the bottles once or twice daily (*i.e.,* in the morning and late afternoon). Replace with a freshly prepared solution every 3 - 5 days.
3. After two weeks, substitute the antibiotic solution with conventional drinking water. Allow a 2-day antibiotic rest period prior to oral infection.
4. Load the *P. gingivalis*/vehicle suspension into a 1 ml tuberculin syringe with an attached feeding needle. Manually restrain the mouse by grabbing the scruff on the back of their neck. Ensure the grip is firm enough to restrict mobility of the mouse's head.
5. Infect mice by topical application of *P. gingivalis* at the buccal surface of the maxillae. Position the feeding needle such that is aligned with the buccal surface of the right maxillary molars and eject 50 ul of bacterial suspension. Disperse the solution gently along the gingiva for 1 min using the ball of the feeding needle.
6. Allow the mouse to rest for a period of 30 sec to 1 min before repeating the procedure on the left maxilla. Control mice receive the antibiotic pretreatment and oral gavage with vehicle alone (2% carboxy methyl cellulose in PBS).
7. To examine pathogen-induced chronic inflammation at local sites induced alveolar bone loss by infecting mice 3 times at 2-day intervals. Sacrifice mice 6 weeks later for evaluation of bone loss by microCT.
8. To examine pathogen-induced chronic inflammation at local and systemic sites, infect atherosclerosis-prone ApoE$^{-/-}$ mice 5 times a week for 3 weeks.

NOTE: Progression of disease in the innominate artery is monitored by serial *in vivo* MRI. Image mice at various time points and sacrifice 6-16 wks later. At the time of sacrifice, assess global atherosclerotic burden by *en face* analysis and determine alveolar bone loss by microCT. Characterize atherosclerotic lesions by histology and immunohistochemistry.

3. Micro-computed Tomography (microCT)

1. Specimen Preparation
    1. Sacrifice mice at the desired time point post-infection. Euthanize mice by CO_2 asphyxation or by another method approved by the institution's animal facility.
    NOTE: Collect blood by cardiac puncture, separate serum, and store at -80 °C for analysis of anti-*P.gingivalis* IgG as described elsewhere[9].
    2. Use a large pair of decapitation scissors to severe the mouse head at the base of skull. Remove the flesh with a pair of forceps and place the skull into a 50 ml conical tube containing 30 ml of 4% buffered paraformaldehyde. Fix the specimen for 24 - 48 hr at 4°C.
    3. Following fixation, rinse the specimen thoroughly with PBS.
    4. Create maxillary block biopsies.
    5. Store the hemi-maxilla in histological grade 70% EtOH at 4 °C until evaluation by microCT.

2. Image Acquisition
    1. Perform image acquisitions using a desktop microCT scanner. Set the X-ray source to a current of 114 µA and a voltage of 70 kV. Load individual hemi-maxillae into the imaging vessel and scan at resolution of 12 µm in all three spatial dimensions.
    NOTE: Load several hemi-maxillae simultaneously within the imaging vessel.
    2. Perform a preliminary low-resolution scan that allows the user to delineate the boundaries for image acquisition and restrict scanning to the region of interest (ROI) using the system.
    NOTE: The intensity of enamel makes the crown of maxillary molars easily distinguishable. Using the molars as a guide loosely set the imaging boundaries to encompass the three molars and the surrounding alveolar bone. This function is also used to discriminate between individual hemi-maxillae when scanning multiple samples within the same vessel.
    3. When scanning is complete, convert the raw image files (.ISQ) into high-quality dicoms (.DCM).

3. Image Analysis
In this protocol, image analysis is performed using a data visualization, processing, and analysis software. First, use morphological landmarks to create a plane of best fit for the cementoenamel junction (CEJ). Then use the to transform the hemi-maxilla into a standard orientation for subsequent measurement of alveolar bone volume.
    1. Open the software and click the "Open Data" icon located in the top left corner of the Pool. Alternatively, use File > Open Data.
    2. Select the DICOM image stack and click Load. The DICOM Loader window appears. Click OK.
    3. Observe the data set as a green icon in the pool. Notice that clicking on the data object causes additional buttons to be displayed in the button area at the top of the Pool. Selecting the icon also causes some information about the data record to be displayed in the Properties Area.
    4. Each icon in the Pool provides a popup menu from which different modules can be selected. Activate the popup menu by clicking on the white arrow in the right hand corner of the data icon. Under the display module, select Isosurface (Display > Isosurface). The Isosurface Icon will appear in the Pool area. When selected, additional settings appear in the Properties Area.
    5. Set the Draw Style to transparent and the Threshold to 2,000. Make sure the compactify and downsample buttons are selected under options. Under Average, ensure x, y, and z are all set to 2. Click Apply to generate the isosurface.
    NOTE: Observe a transparent 3D reconstruction of the hemi-maxilla in the 3D viewer. The benefit of using a transparent draw style for image reconstruction is that the roots of the molars can be easily identified. This will be important when putting the specimen into standard orientation.
    6. Select the green data icon and in the Properties Area select the crop icon. Observe a window displaying the dimensions and coordinates of the data. Set this aside for now. Notice that a bounding box appears in the 3D viewer with green tabs at each corner.
    7. Select the Interact button in the viewer toolbar. Modify the size of the bounding box by clicking and dragging on the green corners. Make sure the box encompasses the region of interest (ROI) and eliminates as much dead space and debris as possible. This will reduce the computational demand on the computer.
    8. Use the Trackball button in the viewer toolbar to rotate the object within the 3D viewer ensuring the ROI is completely encompassed by the bounding box. When satisfied, click OK in the crop window set aside in step 8.
    9. Select the data icon and under the display module select Oblique Slice (OBS). (Display > OBS)
    10. Select the OBS. In the properties area, set the mapping type to linear, the data window range from -200 to 10,000, and sampling to finest. Now select rotate under options. Observe a rotate toggle in the center of the OBS.
    11. Select the interact button in the viewer toolbar and use the handles of the toggle to adjust the cutting plane of the slice. Create a sagittal plane that runs parallel to the roots of the teeth and perpendicular to the occlusal surface of the teeth. The plane should bisect the three molars (M1-M3), as illustrated in **Figure 2**.
    12. Turn off rotate and duplicate the OBS (object>duplicate object). A new OBS appears named OBS 2. Turn on rotate on for OBS 2.
    13. Use the rotate handle to reorient OBS 2 so that it is perpendicular with OBS 1 (see **Figure 2**).
    14. Turn rotate off for OBS 2 and create 3 duplicate slices. These will be name OBS 3, 4, and 5.

4. Picking Points for the Plane of Best Fit
NOTE: Steps 3.4.1-3.4.5 describe the location of 8 points along the CEJ creates a plane of best fit. Choose four of the points from sagittal slices and the other four from coronal slices (see **Figure 3**). When picking points located on sagittal slices in 3.4.6, it may be necessary to adjust OBS 1.
    1. Align OBS 1 with the center of the most mesial root of M1 in the sagittal plane. Align OBS 2 with the center of the most mesial root of M1 in the coronal plane.

2. Align OBS 3 with the center of the bucco-distal root of M1 in the coronal plane. If necessary, adjust OBS 1 so that it is approximately centered with the bucco-distal root of M1 in the saggital plane when selecting points in Step 20.
3. Align OBS 4 with the furcation of the buccal roots of M2. OBS 4 should be centered between the bucco-mesial and bucco-distal roots of M2. If necessary, adjust OBS 1 so that it is approximately centered with the bucco-distal root of M2 in the sagittal plane when selecting points in Step 20
4. Adjust OBS 5 so that it runs down the center of M3 in the coronal plane. If necessary, adjust OBS 1 so that it is approximately centered with the most distal root of M3 in the sagittal plane when selecting points in Step 20.
5. Duplicate any one of the OBSs (OBS 6) and select fit to points in the properties window. The fit to points toggle allows the researcher to pick 3 or more points on 2D or 3D objects within the viewer and then calculates a plane of best fit. In this case, the 2D OBSs described in the previous steps is used to select 8 points along the CEJ.
6. Hide OBS 6 from the 3D viewer by clicking on the orange box in the right hand corner of the data icon. Hide the isosurface from the 3D viewer to make the CEJ visible on all 2D slices. Shift-click and select the 8 points along the CEJ as described above.
   NOTE: If the Shift key is not held down when selecting points, a plane will automatically be calculated after the first three points.
7. After selecting all 8 points, make OBS 6 visible. Note that this is an axial slice that runs approximately parallel to the occlusal plane.

5. Transformation and Reorientation NOTE: The plane of best fit is used to transform the data into a standard orientation for subsequent volumetric measurements.
   1. Click Data Icon>Compute>ApplyTransform. The ApplyTransform icon appears in the Pool Area. Click the white square in the corner of the ApplyTransform icon, select reference, and click on OBS 6.
   2. In the Properties Area, select standard for the interpolation method and extended for mode. Apply the transformation.
   3. Create an isosurface and a coronal OBS for the new data file. Rotate the OBS in the axial direction such that it is approximately perpendicular with M1 (shown in **Figure 2**). Use the cusps of the molar and the occlusal curvatures as a guide.
   4. Use this plane to transform the data as in steps 3.5.1 and 3.5.2. Save the transformed data file.

6. Segmentation and Bone Volume Measurement
   NOTE: The steps below describe the segmentation and measurement of alveolar bone. The slice corresponding to the plane of best fit for the CEJ is identified and a reference plane is chosen. Alveolar bone between the CEJ and the reference plane on the buccal face of the molars is segmented and measured. The most mesial root of M1 and the most distal root of M3 serve as endpoint landmarks. Setting the reference plane 15-20 slices below the CEJ yields optimal results. Inclusion of additional slices introduces variability that masks differences in bone volume among treatment groups.
   1. Open the Segmentation Editor and create a new label for the transformed data.
   2. Create a new material and name it alveolar bone.
   3. Under Zoom and Data Window, set the data range from -200 to 10,000.
   4. Under Display and Masking select the 2D crosshair, 3D MPR, and 3D volume rendering icons. Set the data range from 2,500 to 8,000. Enable data masking.
   5. Select the Four Viewers display setting from the viewer toolbar. The display is divided into four quadrants allowing the simultaneous examination of saggital, coronal, and axial image stacks, as well as the 3D rendered volume.
   6. Use all four quadrants to identify the last slice where enamel is visible on the buccal faces of M1 and M3. This location corresponds to the plane of best fit for the CEJ. Record the axial slice number.
   7. In the axial plane, continue 15-20 slices toward the alveolar bone crest. This represents the reference plane.
   8. Use any combination of segmentation tools to select alveolar bone on the buccal face of the molars between the CEJ and the reference plane. Use the most mesial root of M1 and the most distal root of M3 as endpoint landmarks.
   9. When satisfied, add the selection to Alveolar Bone under the materials list.
   10. Return to the object pool. A new icon with the extension ".Labels" should be appended to the image data icon. Select the Labels icon and in the drop menu select Materials>MaterialStatistics.
   11. In the properties area, select Material and hit apply. A table appears displaying several parameters for each material on the materials list. Record the volume of Alveolar Bone.

4. Assessment of Atherosclerosis

1. Aortic Dissection
   1. Sacrifice the mouse by CO_2 asphyxiation at the desired time point post-infection.
   2. Place the mouse on the dorsal side, tape down and wipe mouse with 70% EtOH. Cut the skin on the ventral side from the middle of the abdomen to just above the xyphoid process.
   3. Cut the abdominal skin until the xyphoid process is visible. Lift the xyphoid process with a small pair of forceps, make cuts on either side of the rib cage, and cut the diaphragm. Then make two cuts down either side of the rib cage to expose the heart.
   4. Exsanguinate the mouse using a 27 G insulin syringe placed into the apex of the right ventricle. During blood collection, periodically rotate the needle to prevent blocking of the opening by the ventricular wall. Typically, 0.8 - 1 ml of blood can be obtained using this method.
   5. sup>NOTE: Separate serum and store at -80 °C for analysis of anti-*P.gingivalis* IgG as described elsewhere[9]
   6. Use scissors to remove the right atrium.
   7. Locate the left ventricle on the posterior side of the heart. Introduce a 21 G needle into the apex of the left ventricle, with the bevel of the needle facing the center of the chamber and slowly flush the circulatory system with 3 - 5 ml of tissue fixative.
   8. Trim fat and thymus surrounding the heart.
   9. Remove the lungs.
   10. Locate the aortic arch with the three branches and clear away surrounding fat layers for better exposure.
   11. Continue dissection of the aorta from the arch to the base of the diaphragm.

12. Remove the liver and displace intestinal tissue to expose the descending aorta. Dissect the distal aorta down to the renal artery branches.
13. Cut the renal arteries and continue the dissection down to the ileal bifurcation.
14. Once the aorta is free from most connective tissues, return to the top of the aorta and snip the very top portion of the three branches off the aorta above the heart.
15. Peel heart upward, snipping underlying fat tissues in order to separate heart from the body.
16. Hold the heart with forceps and pull upward, cutting connective tissue that may still be attached, and continue down to the kidneys and follow down to the legs and snip at lowest point possible.
17. Fix aorta in 10% Formalin for 1 hr with a subsequent PBS wash for 1hr. Alternatively, store aorta in 10% Formalin O/N, rinse in PBS the following day and continue with dissection.
18. Place aorta into a 10 cm petri dish containing PBS.
19. Using a dissecting scope, carefully remove adventitial tissue from the aorta.
20. When aorta is free of excess fat and tissue, cut off bottom two thirds of heart. Start peeling heart muscle away at the end of the heart opposite of the aortic arch. The bulb of the aorta should slowly appear, which will be white in coloration.
21. Continue careful dissection using two forceps until aortic bulbs are free of heart muscle tissue.
22. Place cleaned aorta into a black dissecting tray and cover with PBS.

2. Pinning of Aorta
    1. Keep aorta covered in PBS throughout pinning.
    2. Lay aorta in anatomic position with bulbs of aorta on left.
    3. Place temporary minutien pins at 5 locations starting at 1) top of aorta, 2) below third branch of arch, 3) midway of descending aorta 4) near lower end of descending aorta 5) above branch of femoral artery.
    4. Using extra fine spring scissors, cut up left side of aorta, starting at left branch of femoral artery all the way up to aorta to below lowest branch of ascending aorta.
    5. Cut from leftward side of lowest aortic bulb at the crevice and continue cut to reach intersection of cut along vertical cut of aorta.
    6. Cut across aorta horizontally to reach point of lowest branch of ascending aorta
    7. Cut upwards on right side to above highest branch of aorta.
    8. Cut each branch to expose its inner surface.
    9. Remove some of temporary pins and replace with permanent pins with goal of pinning down all aorta in anatomic location without folding, stretching of aorta. Goal is to expose inner surface of aorta.
    10. Continue pinning until all inner surface of aorta is exposed and clearly visible from above and free of visual interference from pins.

3. Lipid Staining and Lesion Quantification
    1. Prepare Sudan IV staining solution (5 mg/ml in 70% isopropanol). Mix well and filter to ensure no crystals are present.
    2. Cover pinned aorta in Sudan IV solution for 50 min.
    3. Wash with 70% isopropanol for 1 - 5 min. Gently rinse aorta with ddH20 until the water coming off the aorta is no longer red.
    4. Cover aorta with PBS. Capture images of aorta with a high-resolution camera attached to a dissecting microscope and save as digital image files (.TIFF). Place a ruler next to each image to assist in calibration.
    5. Use ImageJ software to determine the area of the intima and area of lesions. Manually trace the intimal surface to determine area. Lesion area can be calculated using automated color thresholding. This requires setting a threshold to define a color intensity that discriminates lesions from normal areas.
    6. Calculate the percentage of the intimal surface covered by atherosclerotic lesions.

5. Histological Assessment of Atherosclerotic Lesions

1. Harvest aortic arch with heart tissue and immerse in O.C.T. in a disposable base mold.
2. Collect 5 µm serial cryosections every 50 µm in the aortic sinus and innominate artery using a cryostat set at -17 °C and mount the tissue sections on microscope slides. Store slides at -20 °C until further use.
3. For histological assessment, stain with hematoxylin & eosin using the appropriate procedures.

6. Immunohistochemical Characterization of Atherosclerotic Lesions.

The steps below outline a general antibody-based protocol routinely employed to assess atherosclerotic lesions in *P. gingivalis*-infected mice. This protocol requires optimization for each antibody or reagent.

1. Remove slides from freezer and fix for 2 min in ice-cold fixative (acetone or other fixative).
2. Allow slides to come to RT and label with a solvent resistant pen.
3. Rinse slides 3x in PBS to remove the tissue-freezing matrix
4. Block endogenous peroxidase activity by incubating the slides in 0.3% H_2O_2 solution in PBS for 10 min.
5. Rinse slides 3x in PBS for 2 min each time.
6. Block non-specific binding by incubating in blocking buffer (10% rabbit serum in PBS) for 30 min at RT.
7. Dilute the primary antibody 1:50 in 10% rabbit serum.
8. Apply the diluted antibody to the tissue sections on the slide.
9. Incubate for 1 hr at RT.
10. Rinse slides 3x in PBS for 2 min each.
11. Dilute anti-rat biotinylated secondary antibody 1:100 in 10% rabbit serum.
12. Apply to the tissue sections on the slide and incubate for 30 min at RT.
13. Rinse slides 3x in PBS for 2 min each.

14. Prepare DAB substrate solution by adding 1 drop of DAB chromogen to every 1 ml DAB buffer.
15. Drain PBS from the slides and apply the DAB substrate solution. Allow slides to incubate for 5 min or until the desired color intensity is reached.
16. Wash 3x in water for 2 min each.
17. Counter stain with hematoxylin.
18. Dehydrate through 4 changes of alcohol (95% 1 min, 95% 1 min, 100% 1 min and 100% 5 min).
19. Clear in 3 changes of xylene.
20. Coverslip using mounting solution and analyze qualitatively by microscopy. For quantitative analysis, acquire images and calculate staining area with ImageJ using an automated threshold.

7. MRI

1. Animal Preparation for MRI
    1. Anesthetize the mice before MRI experiments. Perform the initial induction of anesthesia by using 4% vaporized isofluorane for 2-3 min in an induction chamber. Maintain anesthesia during the imaging period using a continuous flow of 0.5 - 2% vaporized isofluorane delivered through a nose cone setup or mask.
    2. After reaching the surgical plane of anesthesia (*i.e.,* no toe pinch response), place the mouse into an animal holder with its nose inserted into a nose cone. There are several types of commercially available animal holders that can be used to minimize potential movement during imaging. We use a custom designed holder with a bite bar.
    3. Monitor respiration and cardiac cycle and synchronize with image acquisition using a respiration pillow (placed on the mouse's abdomen) equipped with a small animal monitoring and gating system.
    4. Secure the mouse and monitoring system onto the animal holder with laboratory film.

2. MRI data acquisition
    1. Place the animal holder with the mouse's head first in a supine position into a 30 mm vertical probe (Micro 2.5) maintained at 23°C and into the vertical-bore 11.7 T MRI scanner.
    2. Align the holder with the center of the RF coil.
    3. Conduct a shimming process using a single pulse sequence.
    4. Using a RARE sequence, acquire scout images along three orthogonal orientations to create axial, coronal, and sagittal images.
    5. Perform a low resolution Magnetic Resonance Angiography (MRA) using an ungated 3D gradient echo sequence with the following parameters: slab thickness = 1.5 cm; flip angle = 45°; repetition time = 20 ms; echo time = 2.2 ms; field of view = 1.5 × 1.5 × 1.5 cm; matrix = 64 × 64 × 64; number of average = 1. Total scan time: 2#3 min. The purpose of this scan is to ensure that images are acquired at the target region (the innominate artery).
    6. Perform a high resolution MRA of the innominate artery with an ungated 3D gradient echo sequence using the following parameters: slab thickness = 1.5 cm; flip angle = 45°; repetition time = 20 ms; echo time = 2.2 ms; field of view = 1.5 × 1.5 × 1.5 cm; matrix = 128 × 128 × 128; number of average = 4. Total scan time was #25 min.
    7. Obtain continuous axial images of the innominate artery 0.5mm below the subclavian bifurcation.

3. MRI data analysis
    1. Perform image reconstruction and analysis using imaging software associated with the scanner. Achieve the 3D reconstruction of the MRA images by Maximum Intensity Projection.
    2. Use the subclavian bifurcation as an anatomical marker to align data acquired from different mice or the same mouse at different time points. Choose the target cross section of the innominate artery at 0.3- to 0.5-mm distance below the subclavianbifurcation.
    3. Define and calculate luminal area of the chosen cross section with ImageJ. Measurements should be performed in a blinded fashion by two independent observers. Verify measurement reproducibility by calculating interclass correlation coefficients.
    4. For longitudinal studies with serial imaging, normalize luminal area to the area of the lumen obtained at baseline (the very first can in the study) for each mouse. Express the results as change in luminal area over time.
    5. Perform the appropriate statistical analyses (*i.e.,* student t test) to determine significant differences between experimental groups.

Representative Results

Using the appropriate mouse model and oral infection regimen, *P. gingivalis* induces chronic inflammation and immunopathology at local (oral cavity) and systemic sites (arteries) (**Figure 1**).

In mice, oral infection with *P. gingivalis* induces a local inflammatory response that drives the destruction of tooth supporting alveolar bone[8]. *P. gingivalis*-infected mice develop serum antibody responses to this organism that are predominantly of the IgG isotype[9]. Results shown in **Figure 4** are representative of an experiment in which C57BL/6 were infected with *P.gingivalis* three times at two day intervals and sacrificed 6 weeks later for the assessment of alveolar bone loss by microCT. Volumetric analysis using Amira software reveals that *P. gingivalis*-infected mice exhibit significant bone loss compared with uninfected controls (**Figure 4A**). Visual inspection of reconstructed hemi-maxillae illustrates an increase in exposed surface area of the molar roots in infected mice as compared to controls (**Figure 4B** and **Figure 4C**).

In atherosclerosis-prone ApoE$^{-/-}$ mice, *P. gingivalis* induces chronic inflammation that drives alveolar bone loss[12] and inflammatory plaque deposition within the aortic sinus[15] and innominate artery[11]. *P. gingivalis*-induced atherosclerosis occurs as early as 24 hrs following the last infection and can be prevented by immunization prior to infection[16]. Progressive inflammation in the innominate artery of *P. gingivalis*-infected mice can be monitored in live mice by serial *in vivo* MRI at various time points post-infection (**Figure 5**). *En face* measurements of Sudan IV stained aortas demonstrates that *P. gingivalis* infection significantly increases lipid deposition and lesional area on the intimal surface (**Figure 6**). At the time of sacrifice, histology and immunohistochemistry can be used to qualitatively or quantitatively characterize atherosclerotic lesions in the context of cellular composition, the expression of various antigens, and lipid content. Immunohistochemical analysis of aortic sinus lesions

reveals increased macrophage infiltration and elevated expression of the innate immune receptor Toll-like receptor 2 (TLR2) in *P. gingivalis*-infected mice (**Figure 7**).

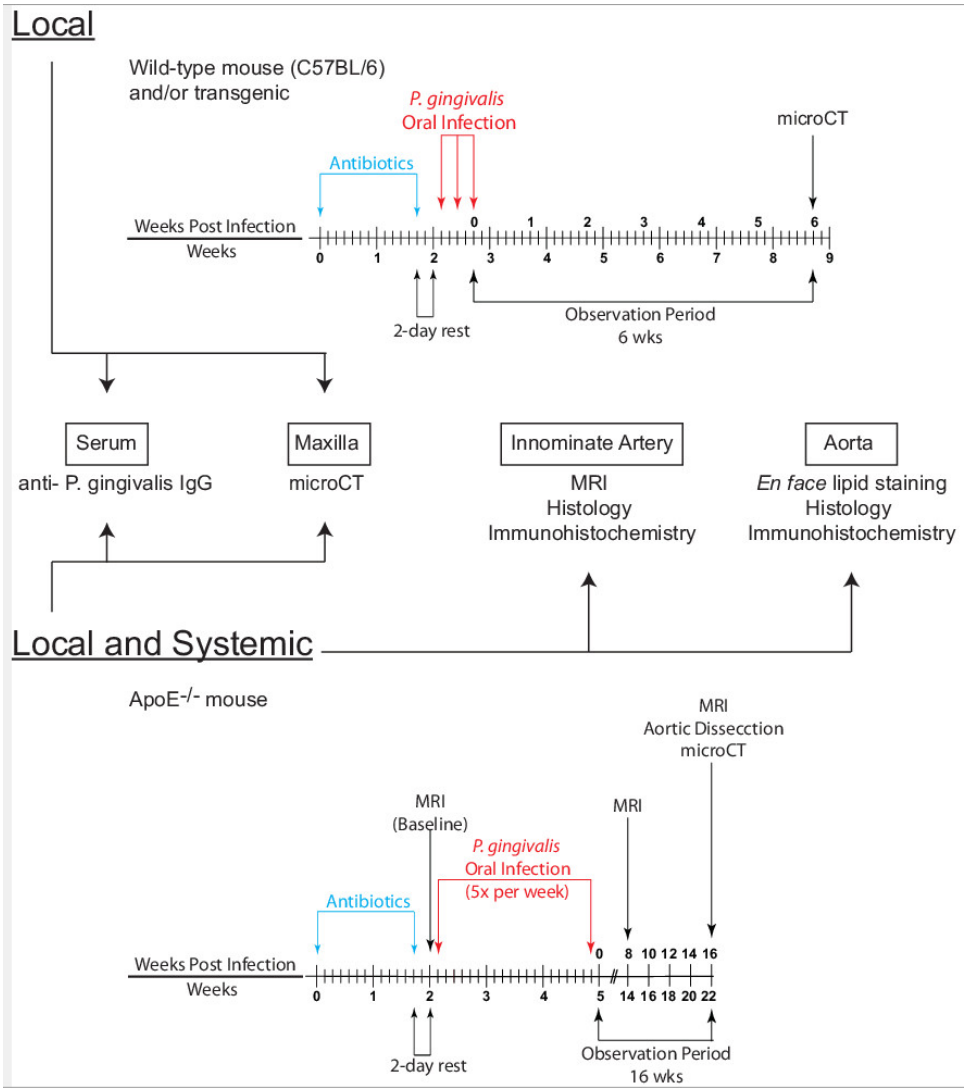

Figure 1. *P. gingivalis*-induced chronic inflammation at local and systemic sites. Prior to infection with *P. gingivalis* mice are administered antibiotics *ad libitum* in their drinking water for 10-14 days followed by a two-day antibiotic rest period. Antibiotic treatment suppresses the indigenous oral flora and facilitates colonization. For the induction of alveolar loss, mice are infected three times at two-day intervals and alveolar bone volume is measured 6 weeks post-infection. When assessing atherosclerosis, atherosclerosis-prone ApoE$^{-/-}$ mice are typically infected 5 times a week for 3 weeks and sacrificed 16-24 weeks post-infection. Progressive inflammation within the innominate artery of live mice can be measured by serial *in vivo* MRI at various time points post-infection. Histology and immunohistochemistry can be used to stain for lipids and inflammatory cells at termination of the experiment to validate imaging data. At the time of sacrifice, alveolar bone loss is measured by microCT and global atherosclerotic burden is assessed by *en face* staining of whole aortas. Please click here to view a larger version of this figure.

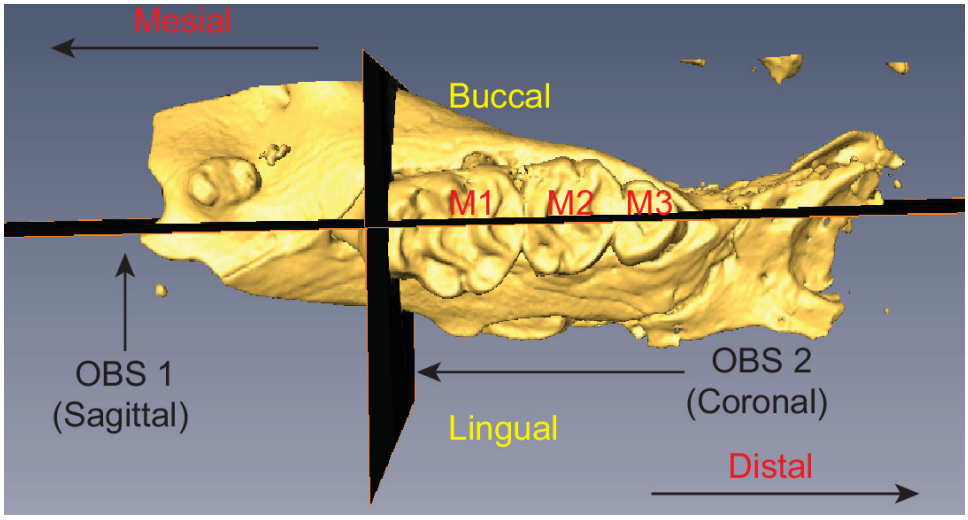

Figure 2. Mouse hemi-maxilla illustrating the positioning of OBS 1 and OBS 2. The three molars are labeled (M1-M3) and relevant anatomically terminology is indicated. Please click here to view a larger version of this figure.

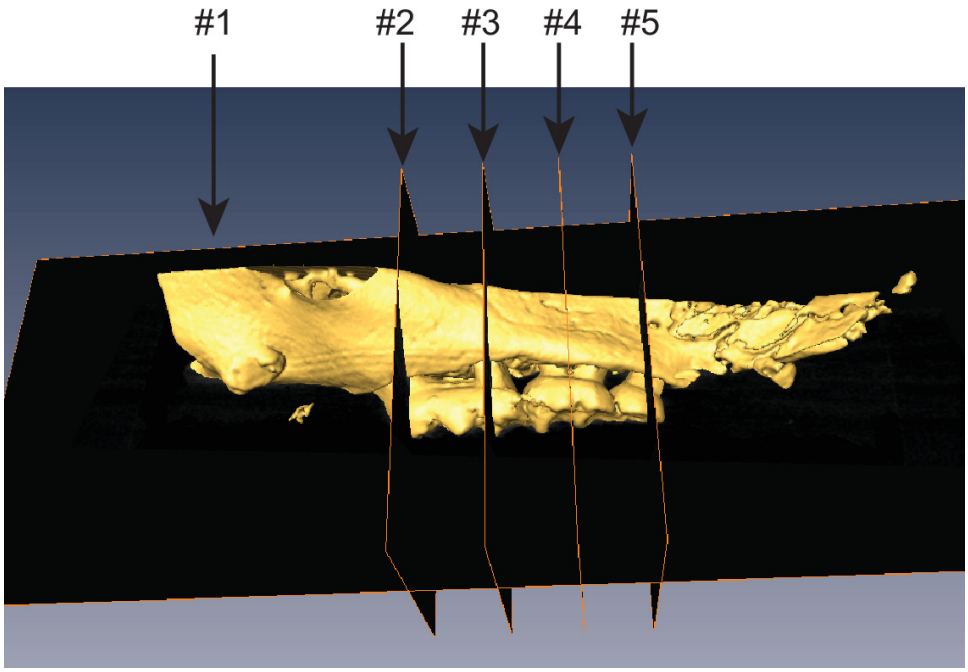

Figure 3. Mouse hemi-maxilla illustrating the positioning of OBS 1 through 5. Please click here to view a larger version of this figure.

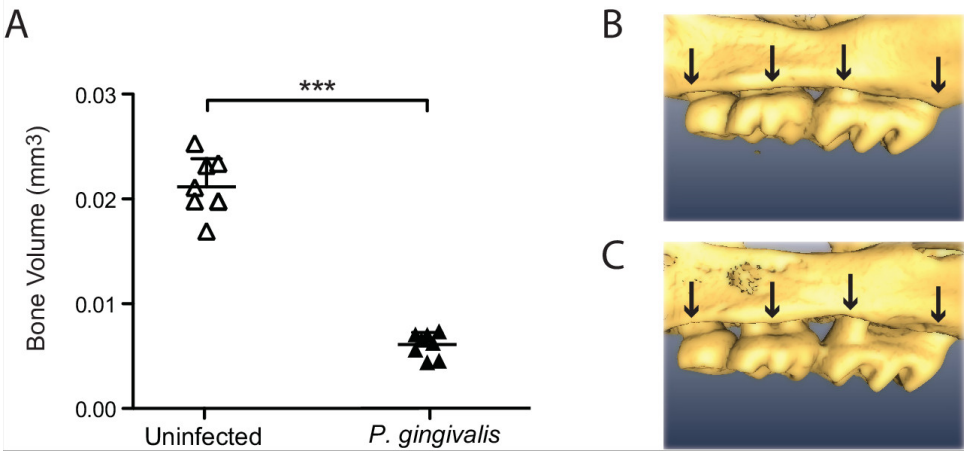

Figure 4. Alveolar bone lossas measured by microCT. Male C57BL/6 were orally infected with *P. gingivalis* or vehicle alone (uninfected) and alveolar bone volume was evaluated by microCT 6 weeks later using Amira. **(A)** Alveolar bone volume in hemi-maxillae from uninfected and *P. gingivalis*-infected C57BL/6. The results represent bone volume above the reference plane (120 microns from the CEJ). Data are expressed as bone volume SD from n=8 mice per group. *** p<0.001, compared to uninfected controls. **(B)** and **(C)** Representative 3D reconstructions of hemi-maxillae from uninfected **(B)** and *P. gingivalis*-infected **(C)** mice. A significant decrease in alveolar bone volume can be seen in *P. gingivalis*-infected mice when compared to uninfected controls. Arrowheads indicate areas where visible bone loss occurs in *P. gingivalis*-infected mice (note the increase in exposed surface area of the molar roots). Please click here to view a larger version of this figure.

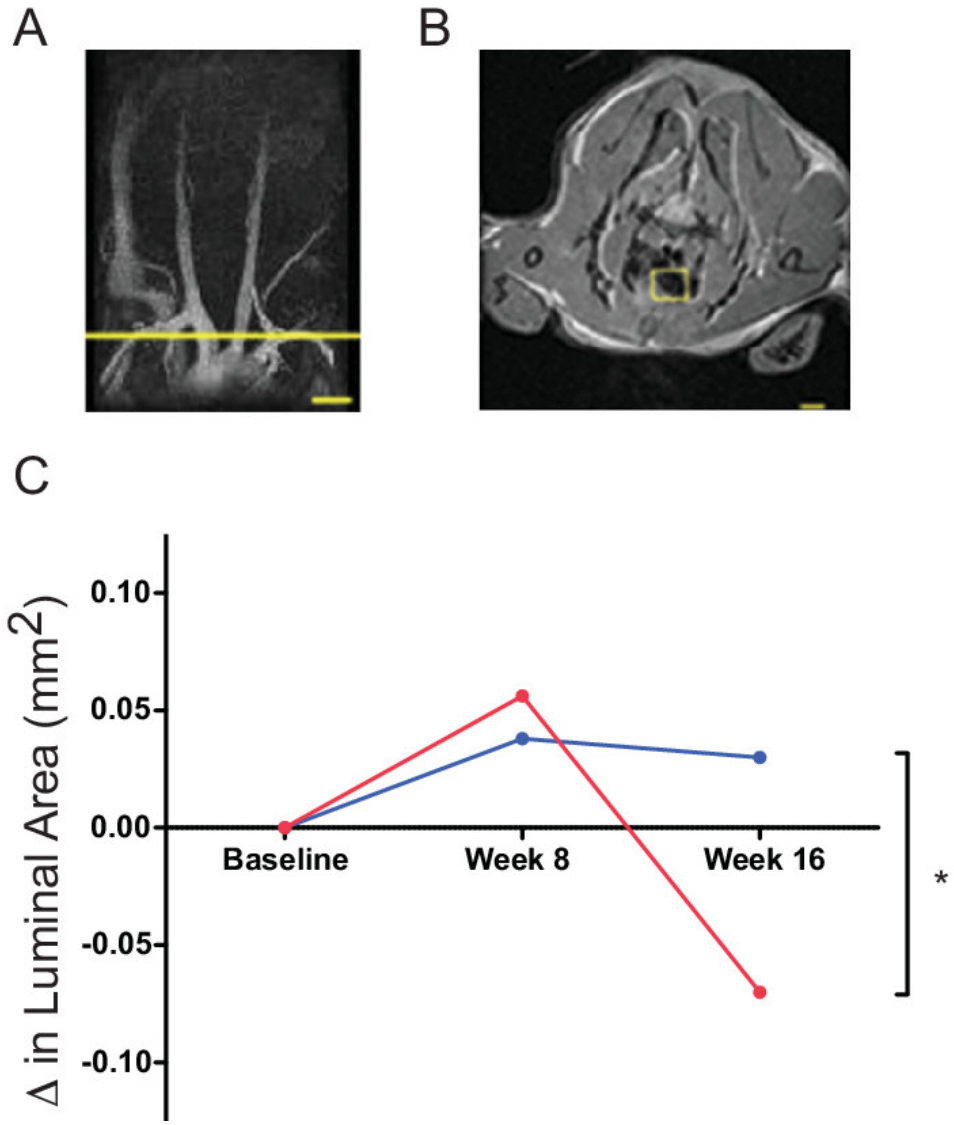

Figure 5. Progressive inflammation within the innominate artery following *P. gingivalis* infection as measured by MRI. (A) Representative Magnetic Resonance (MR) angiogram of aortic arch and major vessels of an ApoE$^{-/-}$ mouse. **(B)** Axial MR image from the yellow line in A of the innominate artery of a mouse, 0.3mm below its bifurcation. Innominate arteries were imaged by MRA at baseline and at 12 and 16 wk post-infection. **(C)** The temporal change in luminal area (mm^2) was calculated for individual mice (*n* = 10-12/group). Uninfected ApoE$^{-/-}$ (blue); *P. gingivalis*-infected ApoE$^{-/-}$ (red). Please click here to view a larger version of this figure.

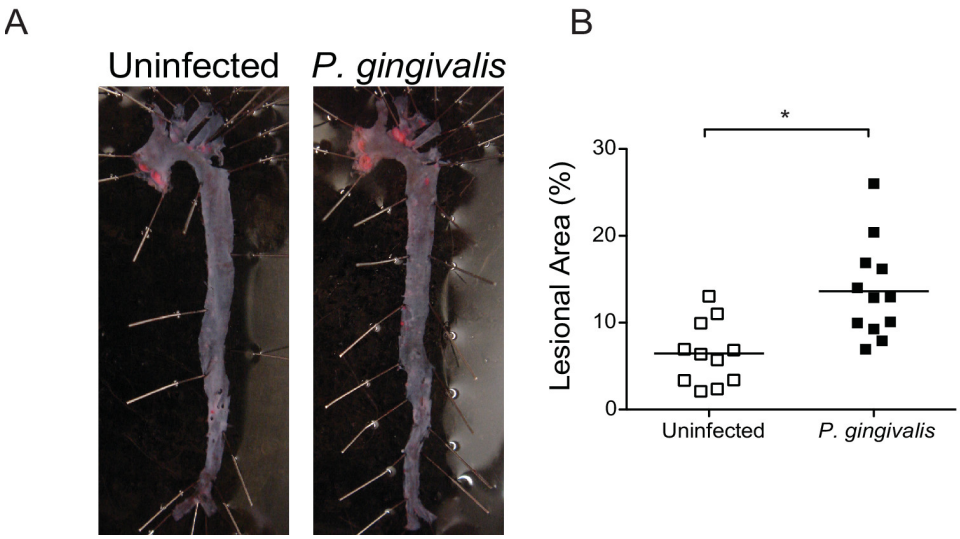

Figure 6. *En face* determination of lesional areain the whole aorta. **(A)** Sudan IV staining of aorta *en face* lesions 16 wk post-infection with *P. gingivalis*. **(B)** Quantification of lipid content within the total aorta of uninfected (white symbols) and *P. gingivalis*-infected mice (black symbols) (*n* = 10–13/group). Percentage of aorta occupied by lipids was calculated using ImageJ. *$p < 0.05$. Please click here to view a larger version of this figure.

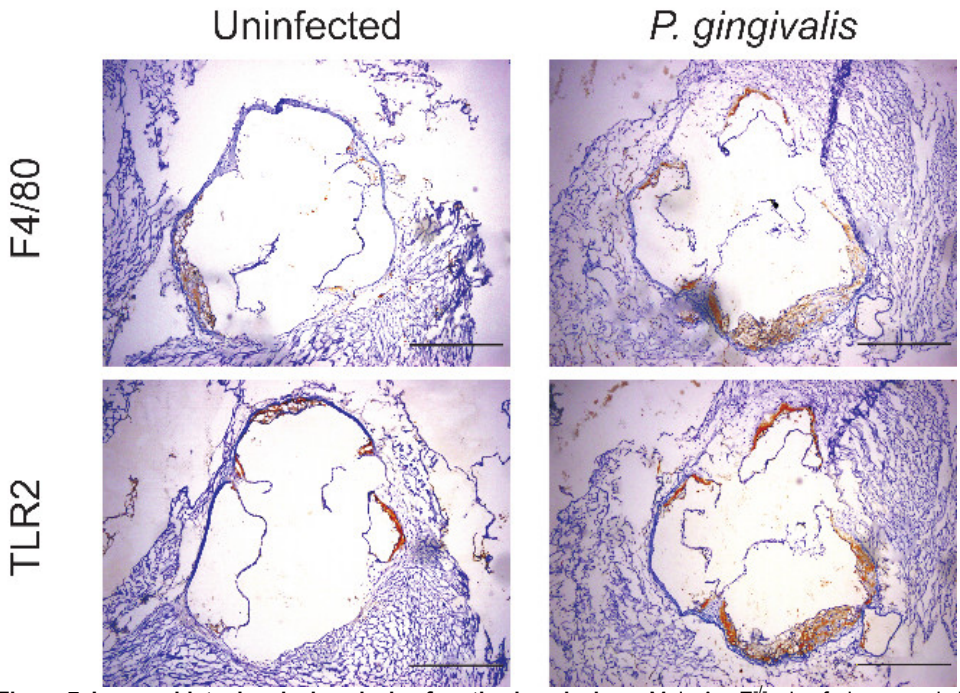

Figure 7. Immunohistochemical analysis of aortic sinus lesions. Male ApoE$^{-/-}$ mice fed a normal chow diet were infected with *P. gingivalis* or uninfected and sacrificed 16 weeks post-infection. Cryosections obtained from the aortic sinus were stained with anti-mouse F4/80 and TLR2. Scale bar, 100 µm. Please click here to view a larger version of this figure.

Discussion

The *P. gingivalis* oral infection model provides a valuable tool for the study of pathogen-induced chronic inflammation at local and systemic sites. This unique model permits the characterization of both host and pathogen specific mechanisms contributing to chronic inflammation and immunopathology. In addition, the model can be used to screen for novel therapeutic strategies, including immunization and pharmacological intervention. The steps outlined in this protocol describe the successful use of this model and detail methodologies to assess the initiation, progression, and outcome of *P. gingivalis*-induced chronic inflammation.

There are several critical aspects to keep in mind when using this protocol to examine inflammatory bone loss. First, it should be noted that the outcome of infection with *P. gingivalis* is determined by three key factors: 1) genetic susceptibility of the host to infection 2) pathogen virulence (genetics of the pathogen) and 3) the resulting host-pathogen interaction (interaction of the two genomes). Susceptibility to *P. gingivalis*-induced alveolar bone loss is genetically determined in mice, thus care must be taken when selecting the strain of mice for study[17]. Differential host

responses among inbred strains of mice can be taken advantage of to conduct forward genetic screens and characterize genes involved in susceptible and resistance to pathogen-induced chronic inflammation. In addition, considerable heterogeneity exists in the ability of different *P. gingivalis* strains to induce alveolar bone loss in mice[18]. This protocol uses mice on the C57BL/6 background because of the availability of transgenic mice and their susceptibility to atherosclerosis. *P. gingivalis* strain 381 induces alveolar bone loss and atherosclerosis in mice on the C57BL/6 background, and several bacterial mutants have been engineered using this strain.

Mice are particularly resistant to atherosclerosis and the development of overt arterial lesions requires the use of genetically modified mouse models of atherosclerosis. We use the ApoE$^{-/-}$ mouse model because it is well-established mouse model of atherosclerosis, does not require feeding of high fat diet for lesion formation, and recapitulates many aspects of human disease[19]. The type of diet to feed the animals during the course of the experiment is an important variable. For the majority of our work, we feed mice a normal chow diet to avoid the contribution of exogenous lipids in the interpretation of our results. In preliminary studies, we found that feeding mice a high fat diet masks differences in *en face* lesion area between uninfected and *P. gingivalis*-infected mice within the aortic sinus. However, high fat diet and *P. gingivalis* infection work synergistically when the progression of inflammation is monitored in the innominate by MRI or histology[11]. In mice, the innominate artery has a high degree of lesion progression, and lesions in this artery express features characteristic of clinical disease in humans including vessel narrowing, atrophic media, perivascular inflammation, and plaque disruption. Distinctions in the cellular composition of lesions are evident at different anatomical sites. Macrophages are the primary immune cells infiltrating aortic sinus lesions, while innominate artery lesions are composed of both macrophages and T cells.

Experimental duration and the time point at which inflammatory endpoints are evaluated are additional factors to consider when assessing initiation, progression, and outcome of *P. gingivalis*-induced atherosclerosis. We previously demonstrated that *P. gingivalis*-infected ApoE$^{-/-}$ mice exhibit macrophage infiltration, elevated expression of innate immune markers, and increased deposition of inflammatory plaque as early as 24h following the last infection within the aortic sinus and this can be prevented by immunization[16]. In our hands, inflammation and immunopathology increase with advancing age and are evident up to 24 weeks post-infection. However, decisions regarding duration of the study ultimately rely on the underlying hypothesis being studied, the mode of analysis and prior knowledge of the extent of atherosclerosis under specific environmental conditions.

The use of non-invasive imaging techniques to monitor progressive inflammation in the innominate artery can be used to guide experimental duration. Serial MRI allows for detailed studies of atherosclerosis progression in the same animal that can depict the narrowing of the arterial lumen and small vessel wall areas[20]. In contrast to traditional methods, such as lipid staining of dissected vessels, MR imaging does not require euthanasia and allows for longitudinal studies to assess the initiation and progression of atherosclerosis. In conjunction with transgenic mice, bacterial mutants, or experimental treatments, the temporal information provided by MRI can be used to evaluate the effect of host genetics, pathogen virulence factors, and therapeutic intervention. As an added benefit, histology and immunohistochemistry can be used to stain for lipids and inflammatory cells at termination of the experiment to validate imaging data. We recently used these methods to demonstrate that oral infection with *P. gingivalis* accelerates atherosclerosis in the innominate arterties of ApoE$^{-/-}$ mice, that immunization provides protection from plaque progression, and correlates with decreases in the accumulation of lipids and inflammatory cells[11].

In summary, this protocol outlines the steps required to produce a robust model of pathogen-induced chronic inflammation, as well as the methods used to assess inflammation at local and systemic sites. Aside from using this model to examine host and pathogen specific mechanisms involved in inflammatory bone loss and atherosclerosis, it can be adapted to study the contribution of pathogen-induced chronic inflammation to additional disease models. This can be accomplished by using transgenic mouse models of disease including rheumatoid arthritis, diabetes, and cancer. Emerging evidence indicates that a number of chronic diseases of unknown etiology may have infectious origins. These diseases include neoplastic, autoimmune, and inflammatory disease, and together compromise the major causes of morbidity and mortality worldwide. Thus, the use of animal models to examine the role of pathogens in diseases driven by chronic inflammation has the potential for broad therapeutic impact and improved diagnostics.

Disclosures

The authors declare that they have no competing financial interests.

Acknowledgements

This work was supported by National Institutes of Allergy and Infectious Diseases Grant P01 A1078894 to C.A.G.

References

1. Nathan, C., & Ding, A. Nonresolving Inflammation. *Cell.* **140** (6), 871-882, (2010).
2. Karin, M., Lawrence, T., & Nizet, V. Innate immunity gone awry: linking microbial infections to chronic inflammation and cancer. *Cell.* **124** (4), 823-835, 2006).
3. Connor, S. M., Taylor, C. E., & Hughes, J.M. Emerging infectious determinants of chronic diseases. *Emerging Infectious Diseases.* **12** (7), 1051-1057, (2006).
4. Barth, K., Remick, D.G., & Genco, C.A., Disruption of immune regulation by microbial pathogens and resulting chronic inflammation. *Journal of Cellular Physiology.* (2012).
5. Hayashi, C., Gudino, C.V., Gibson, F.C., 3rd & Genco, C.A., Review: Pathogen-induced inflammation at sites distant from oral infection: bacterial persistence and induction of cell-specific innate immune inflammatory pathways. *Molecular Oral Microbiology.* **25** (5), 305-316, (2010).
6. Gibson, F.C., 3rd, Ukai, T., & Genco, C.A., Engagement of specific innate immune signaling pathways during *Porphyromonas gingivalis* induced chronic inflammation and atherosclerosis. *Frontiers in Bioscience: a Journal and Virtual Library.* **13**, 2041-2059 (2008).
7. Pihlstrom, B.L., Michalowicz, B.S., & Johnson, N.W. Periodontal diseases. *Lancet.* **366** (9499), 1809-1820, (2005).

8. Baker, P.J., Evans, R.T., & Roopenian, D.C. Oral infection with *Porphyromonas gingivalis* and induced alveolar bone loss in immunocompetent and severe combined immunodeficient mice. *Archives of Oral Biology.* **39** (12), 1035-1040 (1994).
9. Baker, P.J., Carter, S., Dixon, M., Evans, R.T., & Roopenian, D.C., Serum antibody response to oral infection precedes but does not prevent *Porphyromonas gingivalis*-induced alveolar bone loss in mice. *Oral Microbiology and Immunology.* **14** (3), 194-196 (1999).
10. Gibson, F.C., 3rd, Hong, C., *et al.* Innate immune recognition of invasive bacteria accelerates atherosclerosis in apolipoprotein E-deficient mice. *Circulation.* **109** (22), 2801-2806, (2004).
11. Hayashi, C., Viereck, J., *et al. Porphyromonas gingivalis* accelerates inflammatory atherosclerosis in the innominate artery of ApoE deficient mice. *Atherosclerosis.* **215** (1), 52-59, (2011).
12. Hayashi, C., Madrigal, A.G., *et al.* Pathogen-mediated inflammatory atherosclerosis is mediated in part via Toll-like receptor 2-induced inflammatory responses. *Journal of Innate Immunity.* **2** (4), 334-343, (2010).
13. Hayashi, C., Papadopoulos, G., *et al.* Protective role for TLR4 signaling in atherosclerosis progression as revealed by infection with a common oral pathogen. *Journal of Immunology (Baltimore, Md.: 1950).* **189** (7), 3681-3688, (2012).
14. Papadopoulos, G., Weinberg, E.O., *et al.* Macrophage-Specific TLR2 Signaling Mediates Pathogen-Induced TNF-Dependent Inflammatory Oral Bone Loss. *The Journal of Immunology* , (2012).
15. Gibson, F.C., 3rd, Hong, C., *et al.* Innate immune recognition of invasive bacteria accelerates atherosclerosis in apolipoprotein E-deficient mice. *Circulation.* **109** (22), 2801-2806, (2004).
16. Miyamoto, T., Yumoto, H., Takahashi, Y., Davey, M., Gibson, F. C., 3rd & Genco, C. A. Pathogen-accelerated atherosclerosis occurs early after exposure and can be prevented via immunization. *Infection and Immunity.* **74** (2), 1376-1380, (2006).
17. Baker, P.J., Dixon, M., & Roopenian, D.C. Genetic control of susceptibility to *Porphyromonas gingivalis*-induced alveolar bone loss in mice. *Infection and Immunity.* **68** (10), 5864-5868 (2000).
18. Baker, P.J., Dixon, M., Evans, R.T., & Roopenian, D.C. Heterogeneity of *Porphyromonas gingivalis* strains in the induction of alveolar bone loss in mice. *Oral Microbiology and Immunology.* **15** (1), 27-32 (2000).
19. Daugherty, A., Mouse models of atherosclerosis. *The American Journal of the Medical Sciences.* **323** (1), 3-10 (2002).
20. Weinreb, D.B., Aguinaldo, J.G.S., Feig, J.E., Fisher, E.A., & Fayad, Z.A., Non-invasive MRI of mouse models of atherosclerosis. *NMR in Biomedicine.* **20** (3), 256-264, (2007).

